Loading and Release of Small Hydrophobic Molecules in Multilayer Films Based on Amphiphilic Polysaccharides

ARTICLE *in* LANGMUIR · MARCH 2006

Impact Factor: 4.46 · DOI: 10.1021/la052871y · Source: PubMed

4 AUTHORS:

Aurélie Guyomard-Lack
University of Nantes
18 PUBLICATIONS **247** CITATIONS
SEE PROFILE

Bernard Nysten
Université catholique de Louvain
186 PUBLICATIONS **3,325** CITATIONS
SEE PROFILE

Guy Muller
Université de Rouen
12 PUBLICATIONS **301** CITATIONS
SEE PROFILE

Karine Glinel
Université catholique de Louvain
55 PUBLICATIONS **1,799** CITATIONS
SEE PROFILE

Loading and Release of Small Hydrophobic Molecules in Multilayer Films Based on Amphiphilic Polysaccharides

Aurélie Guyomard,† Bernard Nysten,‡ Guy Muller,† and Karine Glinel*,†

UMR 6522, Polymères, Biopolymères, Membranes, CNRS, Université de Rouen, Bd Maurice de Broglie, F-76821 Mont-Saint-Aignan, France, and Unité de Physique et de Chimie des hauts Polymères (POLY), Université catholique de Louvain (UCL), Croix du Sud, 1, B-1348 Louvain-la-Neuve, Belgium

Received October 25, 2005. In Final Form: January 10, 2006

We report on the loading and release behaviors of polyelectrolyte multilayers based on hydrophobically modified carboxymethylpullulan (CMP) derivatives and poly(ethyleneimine) (PEI) toward hydrophobic dye. The dye-loaded films are obtained according to two different protocols: (i) the postdiffusion approach, which involves the diffusion of the dye within preassembled self-assemblies, and (ii) the precomplexation method, which requires the formation of a water-soluble amphiphilic CMP derivative−dye complex before the multilayer buildup. In both cases, we provide clear evidence for the entrapment of the dye in hydrophobic nanoreservoirs resulting from the aggregation of decyl pendent groups grafted on CMP chains. We show that the loading capacity of the multilayers, as well as their release behavior, can be tuned by varying the grafting degree of CMP chains. Moreover, we demonstrate the possibility to trigger the subsequent release of the loaded dye molecules by varying the composition of the surrounding solution.

Introduction

The layer-by-layer (LbL) assembly of oppositely charged polyelectrolytes has been developed in the past decade to prepare ultrathin films.[1,2] The basic principle of this technique consists of the sequential adsorption of polycations and polyanions onto a charged substrate from dilute aqueous solutions. The buildup of the multilayer is at least partly achieved through charge overcompensation after each deposited layer. The LbL technique has aroused considerable attention due to its simplicity, versatility, robustness, and cheapness. In addition, this method allows for control of the film thickness in the nanometer range. Another attractive feature of the LbL technique is the possibility to incorporate a large variety of charged materials to prepare functional films. For instance, inorganic conductive or electroluminescent polymers, nanoparticles, biomacromolecules, dyes, and fullerenes, were successfully incorporated in the films to prepare optical or electronic devices, separation membranes, drug delivery systems, sensors, or antifouling coatings.[3−6] Different strategies were explored to immobilize functional components within the multilayer. One of them consists of the self-assembling of the functional material during the LbL process. For instance, enzymes such as glucose oxidase or peroxidase,[7,8] dyes,[9−12] conductive polyelectrolytes,[13,14] and polypeptides[15] were successfully embedded in polyelectrolyte multilayers. The advantages of this approach include the physical localization of the functional component controlled at nanometer scale. Another route involves the postdiffusion of the functional material within the preassembled polyelectrolyte multilayer. In contrast to the direct self-assembling approach, this process is essentially limited to small molecules which can diffuse into the multilayers. For instance, dyes were successfully incorporated in the films by this way.[16−19] However, both approaches present drawbacks: For instance, the postdiffusion technique is a slow process. Moreover, both routes are limited to water-soluble charged functional components showing a strong affinity to polyelectrolytes. Many applications such as the development of bioactive coatings require a functionalization by hydrophobic materials such as hydrophobic drugs. Recently, a functionalization based on a prodrug approach was described.[20] A prodrug consisting of a hydrophobic drug covalently attached onto a polyelectrolyte chain through a labile succinate ester was embedded in the multilayer. However, this strategy is limited to only a few hydrophobic functional compounds.

Recently, we reported on the preparation of polyelectrolyte multilayers based on amphiphilic anionic polysaccharides.[21] These derivatives were obtained by grafting alkyl chains on carboxymethylpullulan (CMP) precursor (Scheme 1), a flexible anionic polysaccharide. These hydrophobically modified CMPs are well known to develop hydrophobic associations in aqueous solution.[22,23] By inspecting the growth of the multilayers built with

* To whom correspondence should be addressed. E-mail: karine.glinel@univ-rouen.fr. Phone: ++ 33 2 35 14 65 86. Fax: ++ 33 2 35 14 67 04.
† Université de Rouen.
‡ Université Catholique de Louvain.

(1) Schmitt, J.; Decher, G.; Hong, G. *Thin Solid Films* **1992**, *210−211*, 831.
(2) Decher, G. *Science* **1997**, *277*, 1232.
(3) Arys, X.; Jonas, A. M.; Laschewsky, A.; Legras, R. In *Supramolecular Polymers*; Cifferi, A., Ed.; Marcel Decker: New York, 2000; p 505.
(4) Bertrand, P.; Jonas, A. M.; Laschewsky, A.; Legras, R. *Macromol. Rapid Comm.* **2000**, *21*, 319.
(5) Hammond, P. H. *Curr. Opin. Colloid Interface. Sci.* **2000**, *4*, 430.
(6) *Multilayer Thin Films: Sequential Assembly of Nanocomposite Materials*; Decher, G., Schlenoff, J. B., Eds.; Wiley-VCH: Weinheim, 2003.
(7) Lvov, Y.; Ariga, K.; Ichinose, I.; Kunitake, T. *J. Am. Chem. Soc.* **1995**, *117*, 6117.
(8) Caruso, F.; Schuler, C. *Langmuir* **2000**, *16*, 9595.
(9) Ariga, K.; Lvov, Y.; Kunitake, T. *J. Am. Chem. Soc.* **1997**, *119*, 2224.
(10) Fukumoto, H.; Yonezawa, Y. *Thin Solid Films* **1998**, *327−329*, 748.
(11) Nicol, E.; Moussa, A.; Habib-Jiwan, J. L.; Jonas, A. M. *J. Photochem. Photobiol. A* **2004**, *167*, 31.
(12) Tedeschi, C.; Caruso, F.; Mohwald, H.; Kirstein, S. *J. Am. Chem. Soc.* **2000**, *122*, 5841.
(13) Cheung, J. H.; Stockton, W. B.; Rubner, M. F. *Macromolecules* **1997**, *30*, 2712.
(14) Park, M. K.; Onishi, K.; Locklin, J.; Caruso, F.; Advincula, R. C. *Langmuir* **2003**, *19*, 8550.
(15) Etienne, O.; Picart, C.; Taddei, C.; Haikel, Y.; Dimarcq, J. L.; Schaaf, P.; Voegel, J. C.; Ogier, J. A.; Egles, C. *Antimicrob. Agents Chemother.* **2004**, *48*, 3662.
(16) Fahrat, T. R.; Schlenoff, J. B. *Langmuir* **2001**, *17*, 1184.
(17) Klitzing, R.; Möhwald, H. *Macromolecules* **1996**, *29*, 6901.
(18) Nicol, E.; Habib-Jiwan, J. L.; Jonas, A. M. *Langmuir* **2003**, *19*, 6178.
(19) Chung, A. J.; Rubner, M. F. *Langmuir* **2002**, *18*, 1176.
(20) Thierry, B.; Kujawa, P.; Tkaczyk, C.; Winnik, F. M.; Bilodeau, L.; Tabrizian, M. *J. Am. Chem. Soc.* **2005**, *127*, 1626.
(21) Guyomard, A.; Muller, G.; Glinel, K. *Macromolecules* **2005**, *38*, 5737.

10.1021/la052871y CCC: $33.50
Published on Web 02/03/2006

Scheme 1. Anionic Polysaccharide Derivatives Used in This Study[a]

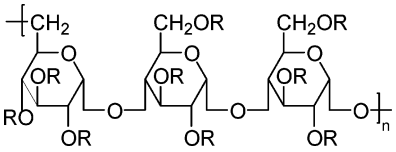

[a] R = H or $CH_2COO^-Na^+$ for CMP precursor and R = H or $CH_2COO^-Na^+$ or $CH_2C(O)OC_{10}H_{21}$ for hydrophobically modified CMPs.

Scheme 2. Nile Red Formula

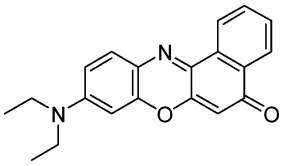

these amphiphilic derivatives and various polycations, we provided evidence for the preservation of the aggregation of amphihilic CMP chains upon adsorption.[21] This result suggests that hydrophobic nanodomains are present in the films. These nanodomains can be regarded as nanoreservoirs for hydrophobic molecules. In the present paper, we probe the presence of these hydrophobic nanodomains in multilayers built with poly(ethyleneimine) (PEI) and CMP derivatives modified by decyl chains by inspecting their ability to trap a hydrophobic dye, Nile Red (Scheme 2). We systematically study the loading and the release behaviors of the films as a function of the amount of hydrophobic decyl chains grafted on the polysaccharide. We also focus our attention on the release behavior of the multilayers as a function of the environmental conditions such as pH and presence of salts.

Experimental Section

Materials. Branched PEI ($pK_a \approx 4-9.5$)[24] (M_w = 750 000 g·mol^{-1}), Nile Red dye, and tris(hydroxymethyl)aminomethane hydrochloride (Tris-HCl) were purchased from Sigma-Aldrich. Sodium chloride (NaCl) and potassium thiocyanate (KSCN) salts were supplied by VWR and were used without any further purification. CMP (Scheme 1) ($pK_a \approx 5$)[25] with a substitution degree in carboxymethyl groups of 0.9 ± 0.05 per anhydroglucose unit and M_w = 235 000 g·mol^{-1} was prepared from pullulan (Hayashibara Biochemical Laboratory, Japan) according to a procedure already described.[26] Hydrophobically modified CMPs (Scheme 1) were synthesized by grafting decyl chains on carboxymethyl groups of the CMP through ester linkage as reported previously.[21,27] Different hydrophobically modified CMP derivatives were obtained by varying the content (from 2 to 18%) of grafted alkyl chains. These derivatives will be denoted CMP-xC$_{10}$ in the following with x the grafting degree defined as the number of decyl chains grafted per 100 anhydroglucose units.

Solutions of Polyelectrolytes. The solutions of polyelectrolytes were prepared by dissolving the polymers in 0.1 M NaCl at a concentration of 2.5 g·L^{-1}. At this concentration, the hydrophobically modified CMP chains were previously shown to form aggregates which are kept upon adsorption.[21] The pH of the solutions was set to 4 and 8.0 by adding 0.1 M HCl or 0.1 M NaOH for PEI and CMP derivatives, respectively. All solutions were filtered through an 8 μm Millipore membrane before use.

Solution of Nile Red. The dye was dissolved in ethanol with a concentration of 2 g·L^{-1}. This alcoholic solution (37.5 μL) was added to 250 mL of Tris-HCl buffer solution (10 mM, pH 7.4) under vigorous stirring. The final solution was stirred for 1 h more at room temperature and filtered through a 0.45 μm Millipore membrane before use.

Preparation of Multilayered Films. The polyelectrolyte multilayers were built on one-side polished (100) silicon wafers (ACM, France) cut into rectangles 3 cm × 1 cm and on SUPRASIL-type fused silica plates (Hellma, France). The substrate was first cleaned by treatment in a hot piranha solution (H_2O_2 (35%)/H_2SO_4 (98%) 1:1 v/v) for 20 min (*caution: piranha solution is extremely corrosive*) and then thoroughly washed with pure Milli-Q water. Multilayers were grown by alternately dipping the substrate in aqueous solutions of PEI and CMP-xC$_{10}$ for 20 min each. Between each deposition step, the substrate was rinsed to remove the excess of polyelectrolyte by dipping the substrate 10 times in three different beakers of pure Milli-Q water and blown dry with a stream of pure air. A film obtained by dipping the substrate N times in the solution of PEI and N times in the solution of CMP-xC$_{10}$ will be named (PEI/CMP-xC$_{10}$)$_N$ in the following.

Loading Experiments. Two different routes have been explored to load Nile Red into the polyelectrolyte multilayers. The first approach involved the postdiffusion of the dye from aqueous solution into preassembled films, while the second one required the "complexation" of the dye with amphiphilic CMP-xC$_{10}$ derivatives before the multilayer buildup.

Loading by Postdiffusion. The films prepared on fused silica slides or silicon wafers were exposed to the Nile Red solution, which was replaced with a fresh one every 2 h. After a given time of immersion, the samples were dipped into three beakers of pure Milli-Q water to remove the dye molecules weakly adsorbed on the surface and dried under a gentle stream of pure air. The dye-loaded films prepared according to this protocol will be denoted (PEI/CMP-xC$_{10}$)$_N$-Nile Red in the following.

Loading by Precomplexation. In these experiments, 10 mg of Nile Red powder was dispersed under vigorous stirring in 10 mL of CMP-xC$_{10}$ solution prepared as described above. This mixture was sonicated for 20 min and vigorously stirred for 12 h more at room temperature. Then, the insoluble part of Nile Red was removed by two ultracentrifugation steps at 70 000 rpm for 1 h at 4 °C. The supernatant containing Nile Red complexed with CMP-xC$_{10}$ derivative was recovered and used to build (PEI/CMP-xC$_{10}$) multilayers. The dye-loaded films prepared according to this protocol will be denoted (PEI/CMP-xC$_{10}$*Nile Red)N in the following. For each loading protocol used, the amount of dye loaded in the films was quantified by performing UV spectroscopy measurements on the dried samples built on quartz slides.

Release Experiments. The dye-loaded films deposited on fused silica slides were immersed into a beaker containing a buffer which was frequently replaced by a fresh one to ensure constant release conditions. The release behavior of the loaded films investigated by UV spectroscopy was studied as a function of the pH and the nature of salts present in the buffer, namely NaCl and KSCN. In this last case, the samples were thoroughly washed with 10 mM Tris-HCl buffer (pH 7.4) and pure Milli-Q water before UV measurements to remove the presence of UV absorbing SCN^- ions in the film.

Characterization Techniques. *UV−Visible Spectroscopy.* The amount of the dye embedded in the multilayer was quantified by UV−visible spectroscopy. The fused silica slides were mounted in a Kontron UVIKON 860 spectrometer sample holder, and the spectra were collected using an uncoated fused silica slide as reference. To ensure the accurate quantification of the amount of Nile Red loaded in the films, the residual absorbance of the polyelectrolyte multilayer was compensated by computing the relative absorbance (A_{rel}) defined as

$$A_{rel} = A_{loaded} - A_{unloaded}$$

(22) Simon, S.; Dugast, J.-Y.; Le Cerf, D.; Picton, L.; Muller, G. *Polymer* **2003**, *44*, 7917.
(23) Duval, C.; Le Cerf, D.; Picton, L.; Muller, G. *J. Chromatogr. B* **2001**, *753*, 115.
(24) Mészáros, R.; Thompson, L.; Bos, M.; de Groot, P. *Langmuir* **2002**, *18*, 6164.
(25) Bataille, I. Ph.D. Thesis, Université de Rouen, 1998.
(26) Bataille, I.; Huguet, J.; Muller, G.; Mocanu, G.; Carpov, A. *Int. J. Biol. Macromol.* **1997**, *20*, 179.
(27) Duval, C.; Le Cerf, D.; Picton, L.; Muller, G. *Colloids Surf., A* **2003**, *220*, 105.

with A_{loaded} and $A_{unloaded}$ the absorbances of dye-loaded and unloaded films, respectively. When reported as absorbance per unit thickness, due care was taken for the presence of films on both sides of the fused silica plates.

Ellipsometry. The thickness of the multilayers grown on silicon wafers was determined by a null ellipsometer from Multiskop instrument (Optrel, Germany) at a fixed angle of 70° and fixed wavelength of 6328 Å. The refractive index of the silicon and the polyelectrolyte films were taken to be $3.882 - j0.019$ and 1.5, respectively. The thickness of the native oxide layer atop the silicon substrate (~15 Å) was systematically subtracted from the computed total thickness of the film.

Atomic Force Microscopy (AFM). Topographic images of the film surface were obtained by AFM under ambient conditions using an Autoprobe CP microscope (Thermomicroscopes, Sunnyvale, CA). The analyses were realized in intermittent contact mode (IC-AFM) using a Pointprobe cantilever from Nanosensors with a free resonance frequencies equal to 170.01 kHz, a spring constant around 50 $N \cdot m^{-1}$, and an integrated silicon tip with a typical apex radius of curvature of about 10 nm. For each sample, square images of different scales were acquired (5×5, 15×15, and 45×45 μm^2). To avoid artifacts due to tip contamination, the tip was cleaned using UV-ozone between each sample.

The images were analyzed as follows. First, they were flattened by subtracting line-by-line a polynome of third degree from the height image. Then, the RMS roughness, R_q, was computed for each image size using the following formula

$$R_q = \frac{\sum (h_i - \bar{h})^2}{N - 1} \quad (1)$$

where h_i is the height of pixel i, $\bar{h}$ is the average height of the image, and N is the total number of pixels in the image.

To refine the analysis of the film morphology, the correlation length, ξ, and the Hurst's exponent, H, characterizing the various surfaces were calculated from the radial power spectral density (PSD), $P(s)$, computed on the whole analyzed scale range.[28] After multiplication by a Welch function,[29] 2D PSDs, $P_{2i}(s_x,s_y)$, were computed for each image as follows

$$P_{2i}(s_x,s_y) = \frac{1}{A_i} \left| \int_{A_i} h_i(x,y)\, e^{2\pi j \cdot (s_x x + s_y y)}\, dx\, dy \right|^2 \quad (2)$$

where A_i is the surface of the image. Circular averaging provided one-dimensional PSDs, $P_i(s)$:

$$P_i(s) = \frac{1}{2\pi} \int_0^{2\pi} P_{2i}(s,\varphi)\, d\varphi \quad (3)$$

After being cleaned up (removal of data points corresponding to the five lower spatial frequencies and to spatial frequencies larger than two-thirds of the Nyquist frequency), the $P_i(s)$'s obtained from different image sizes were merged together after rescaling to obtain for each sample a master $P(s)$ curve spanning a large range of spatial frequencies, s, from 0.1 to 20 μm^{-1} (wavelengths from 50 nm to 10 μm).

The average radial PSDs were fitted with a K-correlation function[30]

$$P(s) = Cste \frac{\sigma^2 \xi^2}{\left(1 + \frac{s^2 \xi^2}{2H}\right)^{1+H}} \quad (4)$$

In this equation, σ is the mean-square roughness of the surface, ξ is known as the correlation length or roughness cutoff length, and H is the Hurst's exponent. ξ controls how far a point on the surface can move before losing memory of the initial value of its vertical coordinate. H characterizes how smooth or jagged the surface is.[31]

Results and Discussion

Loading Behavior of the Films. We first investigate the ability of the (PEI/CMP-xC$_{10}$) multilayers to trap Nile Red by dipping preformed 2-cycle films in a solution of the hydrophobic dye at the concentration of 0.3 $mg \cdot L^{-1}$, which is close to saturation.[32] Nile Red is frequently used to probe the presence of hydrophobic microdomains in amphiphilic polymer[32,33] or protein solutions;[34] it was selected here for its high hydrophobicity (Scheme 2). We used UV−visible spectroscopy on fused silica plates to follow the diffusion of the dye in the films. The thicknesses of the unloaded (PEI/CMP-xC$_{10}$)$_2$ films measured by ellipsometry on silicon wafers were comprised between 35 and 105 Å depending on the grafting degree, x, of the CMP-xC$_{10}$ derivative used for the assembly.[21] As fused silica plates and silicon wafers exhibit essentially similar outer surfaces (amorphous silicon oxide) and considering the limited influence of the nature of the substrate on multilayer growth,[4] we can safely compare results obtained on both types of substrates. Loading experiments performed on a (PEI/CMP-14C$_{10}$)$_2$ sample of 85 Å starting thickness did not show a significant variation of film thickness after being dipped in the dye solution. AFM images of the multilayer recorded before and after 24 h immersion in the Nile Red solution show the presence of a continuous and smooth coating (Figure 1a and b). However, a clear change of the film texture is revealed by the inspection of the ζ value extracted from the radial PSD fits (Figure 1f and Table 1): The ζ value significantly increases after the sample was dipped in the dye solution. Such a change of surface morphology may reflect an increase of domain size rather then an increase of the roughness, as previously observed after the diffusion of the dye into the film.[18]

Figure 2 displays the UV−visible spectra of (PEI/CMP-14C$_{10}$)$_2$ multilayers after different immersion times in the Nile Red solution. The amount of the dye loaded in the film was estimated by measuring the absorbance at 270 nm. The results reported as a function of the immersion time in the Figure 2 (inset) show that the absorbance first increases then reaches a plateau which corresponds to the maximal amount of the dye which can be loaded in the film. Similar loading experiments performed on thicker (PEI/CMP-14C$_{10}$)$_3$ films of 206 Å starting thickness (Figure 2 inset) reveal a continuous increase of the absorbance with the dipping time even after 2 weeks. In fact, this behavior reflects the slow diffusion of the hydrophobic dye into the films: The higher the film thickness, the longer the time to reach the saturation level.

Loading studies were also performed on (PEI/CMP-xC$_{10}$)$_2$ multilayers with x varying from 2% to 18%. The maximal absorbance measured at the plateau for each sample and normalized to the initial thickness of the film is reported as a function of the grafting rate x of the CMP chains in Figure 3. Interestingly, no detectable absorption of the dye was registered for the film based on CMP-2C$_{10}$ even after an immersion time of several days. For higher grafting degrees, x, the maximal absorbance increases linearly with x, which testifies for the diffusion of the hydrophobic dye in the films.

Since the dye is efficiently trapped only by the multilayers built up with amphiphilic CMP derivatives having a grafting

(28) Bollinne, C.; Cuenot, S.; Nysten, B.; Jonas, A. M. *Eur. Phys. J. E* **2003**, *12*, 389.

(29) Press, W. H.; Teukolsky, S. A.; Vetterling, W. T.; Flannery, B. P. *Numerical Recipes in C*, 2nd ed.; Cambridge University Press: Cambridge, 1992.

(30) Palasantzas, G. *Phys. Rev. B* **1993**, *48*, 14472.

(31) Small values of H correspond to extremely jagged surfaces, while larger values of H correspond to surfaces with "smooth" hills and valleys. Thus, H determines the texture of the surface roughness.

(32) Gautier, S.; Boustta, M.; Vert, M. *J. Controlled Release* **1999**, *60*, 235.

(33) Chen, G.; Guan, Z. *J. Am. Soc.* **2004**, *126*, 2662.

(34) Sackett, D. L.; Wolff, J. *Anal. Biochem.* **1987**, *167*, 228.

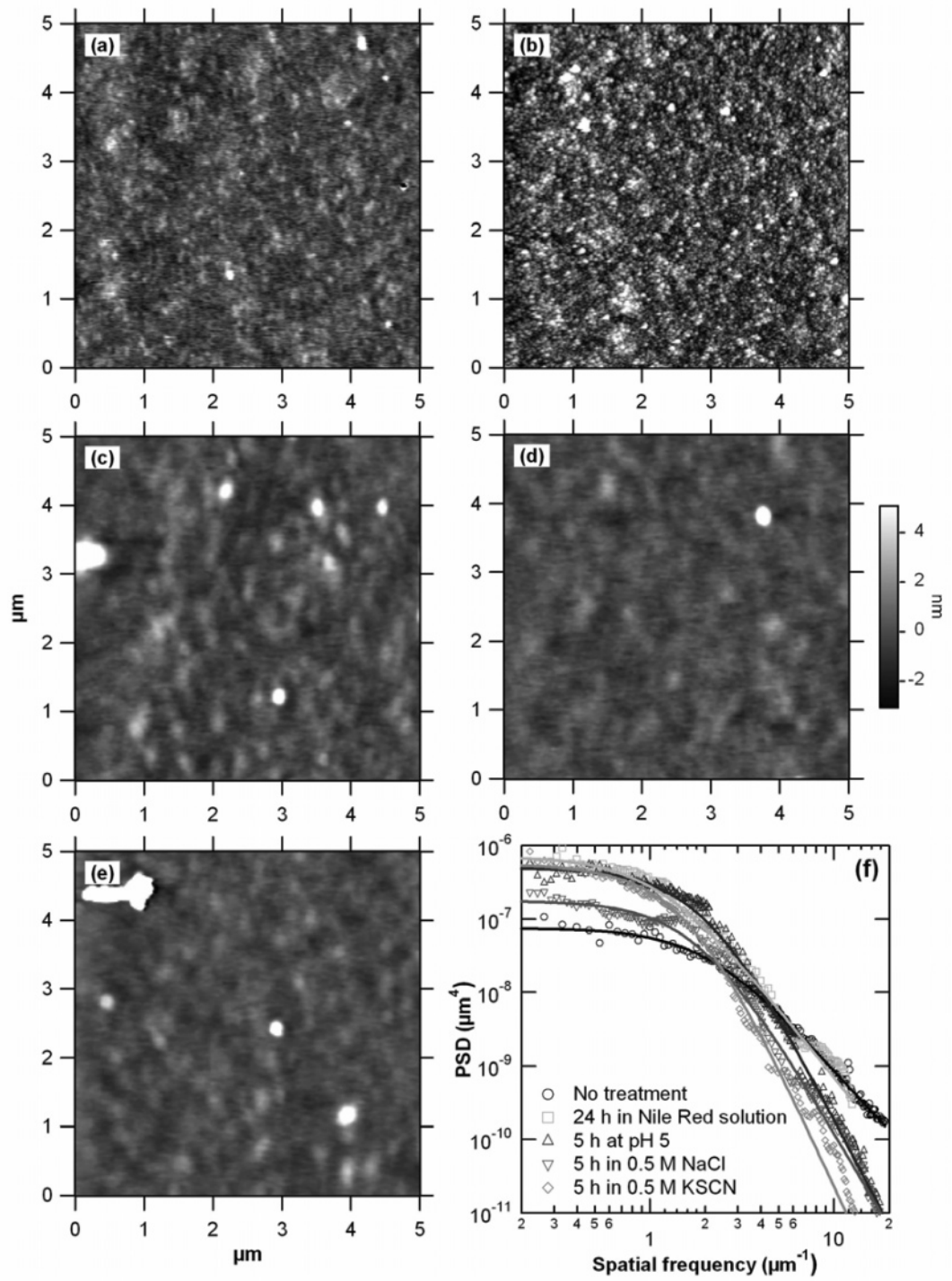

Figure 1. (a−e) $5 \times 5\ \mu m^2$ topographic AFM images of (PEI/CMP-14C_{10})$_2$ samples exposed to different treatments: (a) no treatment, (b) dipping 24 h in Nile Red solution, (c) dipping 5 h at pH 5, (d) dipping 5 h in 0.5 M NaCl, and (e) dipping 5 h in 0.5 M KSCN. (f) Average radial power spectral densities (PSD) calculated for the five samples from the images at 5×5, 15×15, and $45 \times 45\ \mu m^2$; symbols correspond to the experimental data, and solid lines to the fit with the K-correlation function according to eq 4.

degree in decyl chains higher than 2% (Figure 3), we conclude that the ability of the films to load Nile Red is essentially driven by the presence of the hydrophobic pendent chains on CMP macromolecules and not by the residual hydrophobicity of the PEI/CMP polyelectrolyte complex. Moreover, the maximal amount of the dye loaded in the films increases with the grafting degree, *x*, of CMP-*x*C_{10} macromolecules (Figure 3) which supports the presence of hydrophobic nanodomains in the self-assemblies, as evidenced previously.[21] In fact, the hydrophobic aggregates stemming from intra- or intermolecular interactions between decyl chains, and which are formed in CMP-*x*C_{10} solution as demonstrated elsewhere,[21] are most probably kept upon adsorption. Thus, these hydrophobic nanodomains afford suitable sites to trap the hydrophobic molecules: The higher the grafting degree of the CMP derivative, the higher the total volume of the hydrophobic nanodomains in the multilayer and the higher the loading capacity of the film.

To prepare dye-loaded films, we tested a second protocol in which Nile Red was first mixed with the hydrophobically modified CMP derivative in aqueous solution to form a water soluble "complex". This soluble complex was then used to build the multilayers in a second step. This experiment was performed

Table 1. Results of the Analysis of the AFM Images of the (PEI/CMP-14C_{10})$_2$ Samples Exposed to Different Treatments

treatment of the films	RMS roughness[a] (Å)	ξ[b] (Å)	H[c]
no treatment	10	686	0.4
dipping 24 h in Nile Red solution	8	1520	0.6
dipping 5 h at pH 5	12	1331	1.5
dipping 5 h in 0.5 M NaCl	6	1290	1.2
dipping 5 h in 0.5 M KSCN	6	1826	1.8

[a] Roughness calculated on the 5 × 5 μm^2 AFM image. [b] Correlation length obtained from the fits of the average radial PSD (see Figure 1f). [c] Hurst's exponent obtained from the fits of the average radial PSD (see Figure 1f).

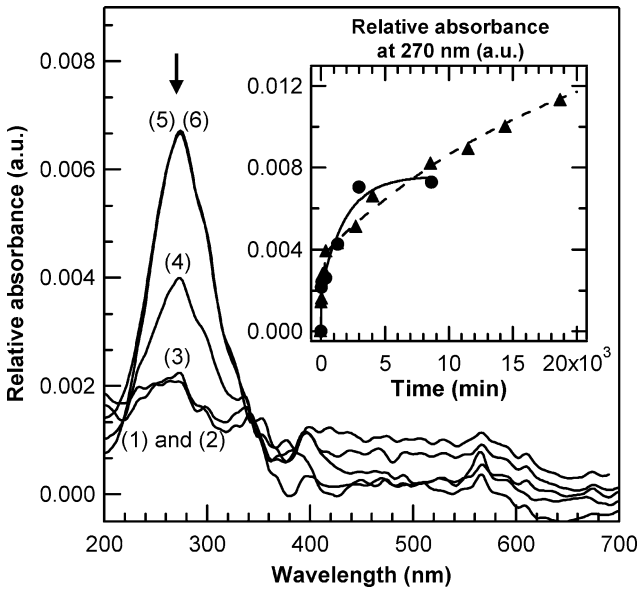

Figure 2. UV spectra of (PEI/CMP-14C_{10})$_2$ films dipped for different times in a Nile Red solution close to saturation. From bottom to top: (1) 30, (2) 70, (3) 370, (4) 1330, (5) 2980, and (6) 8650 min. Inset: Variation of the relative UV absorbance measured at 270 nm versus the time for (PEI/CMP-14C_{10})$_2$ (●) and (PEI/CMP-14C_{10})$_3$ (▲) films.

with the CMP-18C_{10} derivative only, since its complexation capability is higher. To study the ability of this amphiphilic derivative to trap the hydrophobic dye, a control experiment was performed in which a small amount of Nile Red was added into a 2.5 g·L^{-1} CMP-18C_{10} solution upon vigorous stirring at room temperature. The maximal amount of Nile Red solubilized in such conditions was estimated by UV spectroscopy to be 9 mg·L^{-1},[35] which is 30 times higher than the saturation of the dye in water.[32] This behavior confirms the strong ability of the amphiphilic CMPs to trap the dye into hydrophobic nanodomains.

Second, the buildup of the (PEI/CMP-18C_{10}*Nile Red)$_N$ films based on the (CMP-18C_{10}*Nile Red) complex was investigated simultaneously by ellipsometry and UV spectroscopy. The variation of the thickness of the film with the number of dipping cycles presented in Figure 4a shows a continuous multilayer growth in agreement with the previous study reported without dye.[21] Therefrom we can conclude that the complexation between CMP-18C_{10} and Nile Red does not induce a significant perturbation of the LbL deposition. The increase of the absorbance measured at 270 nm with the number of dipping cycles (Figure 4b) provides the evidence for the continuous loading of the dye during the multilayer growth. Interestingly, this would not be the case if electrostatic interactions were used as driving force instead

(35) This concentration was estimated from UV absorbance of the (CMP-18C_{10}*Nile Red) solution measured at 270 nm and the extinction coefficient of the Nile Red ϵ_0 = 0.02 L·mg^{-1}·cm^{-1} determined in aqueous solution.

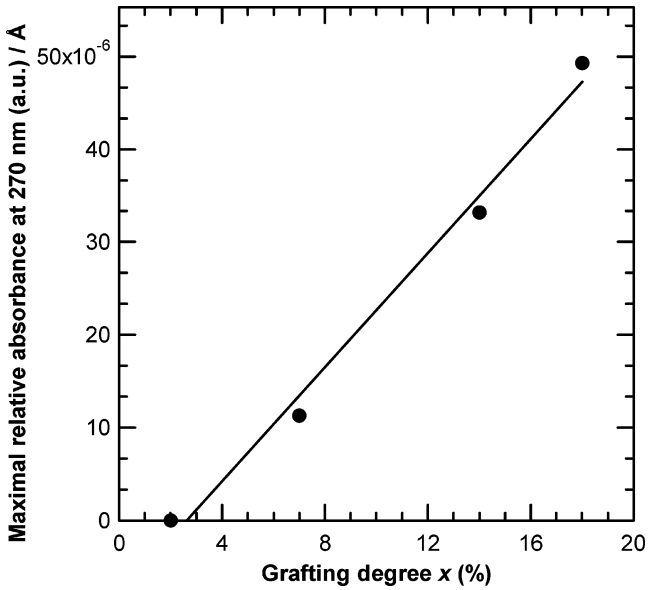

Figure 3. Variation of the maximal relative UV absorbance per Å measured at 270 nm for dye-loaded (PEI/CMP-xC$_{10}$)$_2$-Nile Red films based on CMP-xC$_{10}$ derivatives of varying grafting degree, x. The line is a fit to the data.

of hydrophobic ones, as reported by Jonas et al.[18] who showed that a cationic water-soluble dye complexed by a polyanion is systematically released from the film during the subsequent deposition of a polycation. In contrast, in our case, the dye remains trapped in the hydrophobic nanodomains once the complex is adsorbed on the surface. The relative UV absorbance determined per Angström of film is ~7.6 10^{-6} for (PEI/CMP-18C_{10}*Nile Red) films (Figure 4), which is lower than the value of 4.9 10^{-5} obtained for postloaded (PEI/CMP-18C_{10})-Nile Red samples (Figure 3). Thus, the postdiffusion process is more efficient to dope the films. However, it is a slow process which can require several days (Figure 2), whereas the precomplexation protocol has the advantage to be faster which makes it more attractive for a potential application.

Release Behavior of the Films. The release behavior of dye-loaded (PEI/CMP-xC$_{10}$)$_2$ films was first investigated in pure water. However, no significant release was noticed in water even after a dipping time of several days. Thus, the release of the dye is dramatically slowed and cannot be observed in the selected experimental time window due the strong affinity between Nile Red molecules and hydrophobic nanodomains present in the films.

Several papers reported on the successful release of guest molecules embedded in weak polyelectrolytes multilayers or encapsulated in weak polyelectrolyte capsules upon variation of external pH or ionic strength.[12,36−41] While the variation of pH results in a change of the number of effective charges on weak polyelectrolyte chains, the presence of small ions is known to weaken electrostatic bonds between polyelectrolytes. In both cases, such changes are accompanied by the formation of pores within the films which accelerates the release of the guest molecules. To test the efficiency of the Nile Red entrapment, we

(36) Kharlampieva, E.; Sukhishvili, S. A. *Langmuir* **2004**, *20*, 9677.
(37) Sukhorukov, G. B.; Antipov A. A.; Voigt, A.; Donath, E.; Mohwald, H. *Macromol. Rapid Comm.* **2001**, *22*, 44.
(38) Qiu, X.; Leporatti, S.; Donath, E.; Möhwald, H. *Langmuir* **2001**, *17*, 5375.
(39) Chung, A. J.; Rubner, M. F. *Langmuir* **2002**, *18*, 1176.
(40) Antipov, A. A.; Sukhorukov, G. B.; Möhwald, H. *Langmuir* **2003**, *19*, 2444.
(41) Burke, S. E.; Barrett, C. J. *Macromolecules* **2004**, 37, 5375.

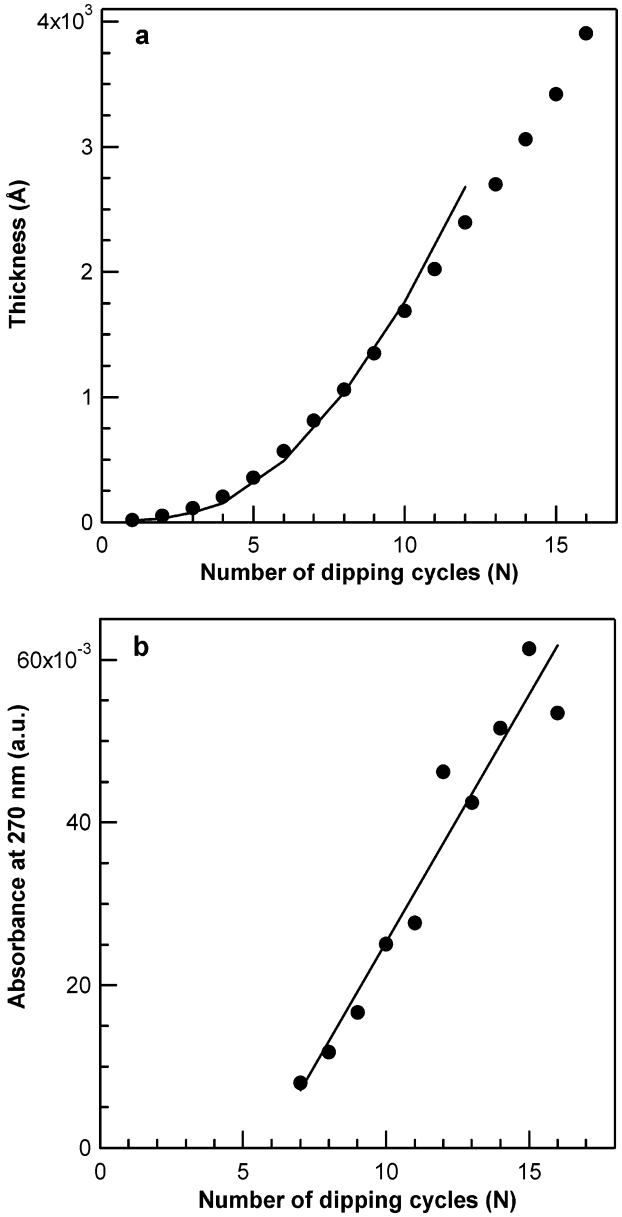

Figure 4. (a) Variation of the thickness of the (PEI/CMP-18C_{10}*Nile Red)$_N$ films loaded by precomplexation as a function of the number of dipping cycles. The line represents the multilayer growth obtained without Nile Red and reported in ref 21. (b) Variation the UV absorbance of the (PEI/CMP-18C_{10}*Nile Red)$_N$ films as a function of the number of dipping cycles. The line is a fit to the data. Below $N = 7$, the absorbance due to the dye was too weak as compared to the absorbance due to the film, and is thus not reported.

investigated the release behavior of our dye-loaded films against such variations of external conditions. We first focused on the influence of the pH on the release behavior of the (PEI/CMP-xC$_{10}$)$_2$-Nile Red films loaded according to the postdiffusion process. The samples were dipped in buffer solutions of fixed pH's comprised between 5 and 7.4. The ellipsometry measurements performed on unloaded multilayers before and after an immersion time of 24 h did not show a significant variation of the thickness, which demonstrates that the films are stable toward the tested media. The AFM measurements performed on (PEI/CMP-14C_{10})$_2$ sample exposed 5 h to pH 5 (Figure 1c) reveals that the film remained homogeneous without the apparition of holes. A clear change of the film morphology was observed, as illustrated by the higher ζ and H values (Table 1). These observations confirm that the internal structure of the film is

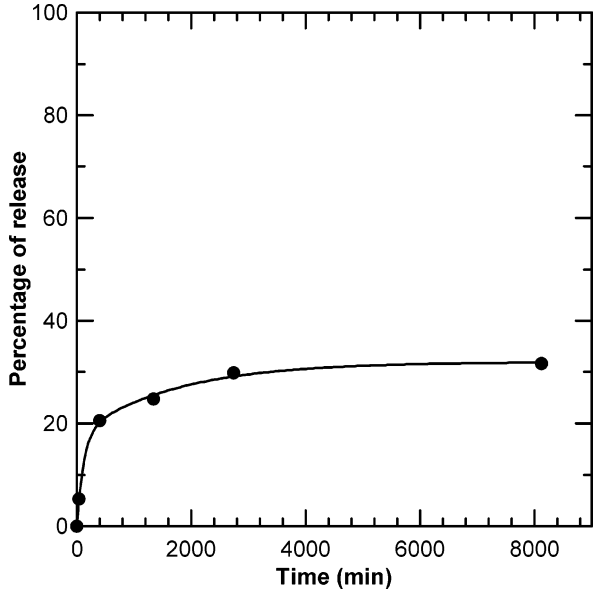

Figure 5. Percentage of dye released from (PEI/CMP-14C_{10})$_2$-Nile Red film loaded by postdiffusion and immersed in solution of pH 5.

Table 2. Percentage of Dye Released from (PEI/CMP-xC$_{10}$)$_2$-Nile Red Films Loaded by Postdiffusion and Immersed in Solutions of Different pH's

	percentage of release		
Nile Red-loaded sample	pH 7.4	pH 6	pH 5
(PEI/CMP-7C_{10})$_2$	–	–	38
(PEI/CMP-14C_{10})$_2$	0	13	32
(PEI/CMP-18C_{10})$_2$	–	–	4

affected by the treatment at pH 5 which is close to the pK_a of the CMP derivative. The typical release profile obtained for (PEI/CMP-14C_{10})$_2$-Nile Red sample immersed in solutions of pH 5 is displayed in Figure 5. As seen, the percentage of release first increases, then reaches a plateau corresponding to the maximal percentage of release. The maximal percentages of the dye released from the (PEI/CMP-xC$_{10}$)$_2$-Nile Red samples dipped in solutions of different pH's are reported in Table 2.

No desorption of the dye is observed at neutral pH for (PEI/CMP-14C_{10})$_2$-Nile Red films, even after an extended dipping time of several days. For lower pH's, the percentage of the released dye slightly increases to reach about 30% at pH 5. It is difficult to provide a detailed picture of the very complex inner balance of forces within the film, which involves pairing of charges and hydrophobic interactions, depending on the partial protonation of carboxylic acid moieties. However, one may speculate that the partial release reflects a complex distribution of dye molecules in the film: Whereas a small part of Nile Red molecules is weakly trapped in the polyelectrolyte complex outside hydrophobic nanodomains and will be released by a variation of pH, a larger part is certainly trapped within hydrophobic aggregates whose structure is essentially not affected by the pH variation. Similar studies performed at pH 5 with (PEI/CMP-18C_{10})$_2$-, (PEI/CMP-14C_{10})$_2$-, and (PEI/CMP-7C_{10})$_2$-loaded films (Table 2) clearly show that the amount of released dye decreases with increasing grafting degree, x, supporting our speculation. Similar results (data not shown) were obtained for the samples loaded according to the precomplexation protocol.

In a second step, we investigated the addition of two different salts in the dipping solution, namely KSCN and NaCl, on the release behavior of the loaded films. In solution, the chaotropic KSCN salt has the property to disrupt the water structure by

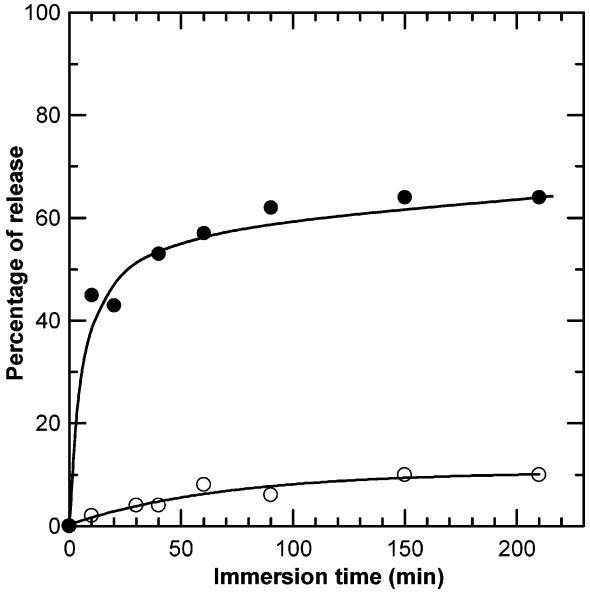

Figure 6. Percentage of dye released from (PEI/CMP-14C_{10})$_2$-Nile Red films loaded by postdiffusion and immersed in 0.5 M NaCl (○) and 0.5 M KSCN (●) solutions (pH 7).

breaking up hydrogen bonds and promotes the disruption of hydrophobic interactions.[42−44] In contrast, the NaCl salt is known to be a lyotropic salt, decreasing the solubility of apolar moieties and consequently reinforcing the hydrophobic interaction.[42−44] Figure 6 displays the release profiles of two (PEI/CMP-14C_{10})$_2$-Nile Red films dipped in 0.5 M NaCl and 0.5 M KSCN solutions, respectively. Whereas the maximal percentage of release obtained in 0.5 M NaCl was about 10%, it reached 65% in 0.5 M KSCN. The thickness of the unloaded (PEI/CMP-14C_{10})$_2$ sample was measured by ellipsometry before and after incubation in 0.5 M NaCl and 0.5 M KSCN solutions, respectively. In both cases, no significant variation of the film thickness was detected (results not shown), even after several hours, which testifies for the film stability in these media. The film morphology was observed by AFM (Figure 1d and e). At all scales, the film remained homogeneous without hole or pit, but the morphology changed after salt treatment with a significant increase of ζ and H values (Table 1). This obviously indicates that the films reorganize upon immersion in salted solutions due to a change in the balance of electrostatic forces. However, whereas NaCl fails to disrupt the hydrophobic domains due to its lyotropic nature, the chaotropic KSCN promotes a significant disruption of these domains, as testified by the much larger dye release observed. While this experiment confirms the existence of hydrophobic domains in the films, it also suggests that the addition of a chaotropic salt could be elegantly used to release efficiently an active hydrophobic component from the films.

Conclusion

We showed that the use of amphiphilic polysaccharides as film constituents represents an elegant way to form hydrophobic nanoreservoirs which are able to trap small hydrophobic molecules. The tunable hydrophobicity of the hydrophobically modified polysaccharides offers a convenient way to control the number of hydrophobic nanocontainers in the films and consequently their loading capacity. In addition, we demonstrated the possibility to trigger the subsequent release of the loaded molecules by varying the composition of the surrounding solution. This approach could be applied to prepare smart coatings for trapping and releasing hydrophobic drugs. Further research is underway to develop such functional thin films.

Acknowledgment. The research was financially supported by "Réseau Normand Matériaux Polymères, Plasturgie" and by European INTERREG IIIA program (AMACOM project). B.N. is a Research Associate of the Belgian National Funds for Scientific Research (FNRS).

LA052871Y

(42) Collins, K. D.; Washabaugh, M. W. *Q. Rev. Biophys.* **1985**, *18*, 323.
(43) Kabalnov, A.; Olsson, U.; Wennerström, H. *J. Phys. Chem.* **1995**, *99*, 6220.
(44) Picton, L.; Muller, G. *Prog. Colloid Polym. Sci.* **1996**, *102*, 26.